# CHAPTER 5

## Raman analysis of red-brown and gray shards from 16th and 17th century Portuguese shipwrecks

**The chapter contains an article published in "Crystal Engineering"**

Available online at www.sciencedirect.com
SCIENCE DIRECT®

Crystal Engineering 6 (2003) 287–299

Crystal Engineering

www.elsevier.com/locate/cryseng

# Raman analysis of red-brown and gray shards from 16th and 17th century Portuguese shipwrecks

M.A. Legodi, D. de Waal *

*Department of Chemistry, University of Pretoria, Pretoria 0002, South Africa*

Received 19 December 2003; accepted 10 April 2004

**Abstract**

The artifacts under investigation (three red clay shards, two gray clay shards and a red clay teapot) are from the J A Van Tilburg museum at the University of Pretoria (UP). The large red clay shard was recovered from the 1552 Portuguese shipwreck, São João, found in the region of Port Edward, South Africa. The other shards were recovered from the 1622 Portuguese shipwreck, the São João Baptista, which sank around Kenton-on-sea off the South African coast. The results from these are compared to those obtained from the analysis of a red-brown teapot. The oldest of this type of teapot was made in China during the second half of the 18th century. Raman spectroscopy has proven to be a useful tool for qualitative determination of the composition of these clay artifacts. The red clays were characterized by the presence of hematite, kaolin, quartz, amorphous carbon and aluminosilicates. The results of the clay teapot differed from those of red clay shards in that no quartz Raman bands were observed for the clay teapot. The gray clay shards were characterized mainly by the presence of quartz, kaolin, amorphous carbon and aluminosilicates. The presence of mullite in all samples could not be ascertained unambiguously using Raman spectroscopy. The pigments found in the investigated samples are hematite ($\alpha$-$Fe_2O_3$) (for red samples) and amorphous carbon (for both red and gray samples).


*Keywords:* Raman; Shipwreck; Clay shard; South Africa; China

* Corresponding author. Tel.: +27-12-4203099; fax: +27-12-3625297.
*E-mail address:* danita.dewaal@up.ac.za (D. de Waal).

1463-0184/$ - see front matter 
doi:10.1016/j.cryseng.2004.04.005

## 1. Introduction

The red iron oxides were widely used as pigments since antiquity because of their rich variety of shades and for the fact that they are not fugitive. Moreover, these pigments are highly variable in texture, lustre and hardness [1]. The red iron oxides ($\alpha Fe_2O_3$) are the most thermally stable of all iron oxide pigments [2]. They could be acquired during firing from siennas (FeOOH) or added to starting materials such as red ochre or synthetic hematite. These oxides also occur in soils and are normally mixed with a variety of clay minerals, e.g. kaolins.

The identification of pigments on artworks are important for conservation and restoration, characterization of materials, dating and authentication [3].

The most important clay minerals reportedly used in China since ancient times are the kaolin group minerals [4] and are also referred to as 1:1 phyllosilicates. They are layered silicates with the form 1:1 t–o (tetrahedral–octahedral) layered structures, and are triclinic [5]. Kaolin is a group of minerals with particles predominantly $<2$ μm in size, neutral and thus chemically stable. This group includes kaolinite, halloysite, nacrite and dickite all with the same chemical formula, $Al_2Si_2O_5(OH)_4$, but differing in structure and arrangement of aluminosilicate layers in the unit cell [4,5]. It is rare to find dickite and nacrite because these occur in small quantities in nature [6]. Kaolinite and halloysite are commercially significant and are used separately or as mixtures. These generally form the highest percentage of the clay used in making artifacts, because they are readily available in nature [6]. Kaolins are the major starting materials in the production of clay wares [7]. During firing at higher temperatures (above 1200 °C) these are transformed into mullite ($3SiO_2{\cdot}2Al_2O_3$) [8]. The presence of kaolins in the finished product suggests that the artifact was not fired at high enough temperatures to effect complete phase transformation [7].

Quartz ($\alpha$-$SiO_2$) is normally part of raw materials used in clay pottery making. It occurs in the form of sand particles, pebbles or flint [9]. During high temperature firing, it is converted into tridymite or cristobalite depending on the form of quartz used [8]. For instance, cristobalite is formed when flint is fired at higher temperatures (1070 °C). To obtain vitrification of the silicium and flux present in the clay, very high temperatures are required around 1100–1300 °C [10]. These are the temperatures at which cristobalite and tridymite are formed from quartz. The observance of quartz peaks in the finished product and absence of its higher temperature phases (above) show that the object was not fired at high enough temperatures to transform its particles. Quartz peaks may be overshadowed by the broad bands of high content of amorphous aluminosilicates (e.g. glassy phase). The small amount and crystal size of quartz may make it difficult to detect its bands in the Raman spectrum [11,12].

As a non-destructive technique, Raman spectroscopy does not require any sample preparation [13]. Raman spectroscopy with its high reliability, sensitivity and specificity [14] has become the instrument of choice when analyzing archaeological artifacts and pigments on art works [15]. It probes those vibrational transitions involving polarizability changes.


Fig. 1. The ceramic artifacts analyzed (sample nos. 1–6). Sample no. 1 was recovered from the São João shipwreck, nos. 2–5 from São João Baptista shipwreck and no. 6 is a ceramic teapot originating from the 19th century China.

A number of artifacts kept in the Van Tilburg Museum at University of Pretoria were recovered from two shipwrecks off the South African coast. The Portuguese ships were from Asia en route to Europe. The artifacts under investigation included three red clay shards, two gray clay shards and a clay teapot shown in Fig. 1. The large red clay shard (no. 1) was recovered from the 1552 shipwreck, of the Portuguese ship called São João, which sank around Port Edward off the South African coast. The other shards were recovered from the 1622 Portuguese shipwreck, the São João, which sank around Kenton-on-sea off the South African coast. The clay teapot was made in China during the 18th century [10]. Due to the historic value of these samples, they need to be handled with care. Furthermore, the colouring materials for all samples seem to have been mixed entirely with the bulk material and not applied only on the surface.

The main objective of this study was to determine the composition of the above-mentioned clay artifacts and to investigate the presence and types of pigments (particularly the iron oxides) used for red and black colouring. The study will further contribute to the realization of Raman spectroscopy as a tool in the analyses of ceramic artifacts. The results obtained here will then be deposited to a database of ancient Chinese clay artifacts.

Table 1
List of the names, origins and descriptions of clay samples analyzed

| Figure name | Origin | Description |
|---|---|---|
| Fig. 1, no. 1, large red clay | São João | Red with white tinge, small dents around body. |
| Fig. 1, no. 2 round red clay | São João Baptista | Red with white tinge, small dents around body. |
| Fig. 1, no. 3 small red clay | São João Baptista | Red with white tinge, small dents around body. |
| Fig. 1, no. 4 large gray clay | São João Baptista | Gray and black, small dents around the body. |
| Fig. 1, no. 5 small gray clay | São João Baptista | Gray and black, small dents around the body. |
| Fig. 1, no. 6 red clay pot | Chinese origin | Deep bright red. |

## 2. Experimental

### 2.1. Samples

The samples analyzed are shown in Fig. 1 and described in Table 1.

### 2.2. Raman spectroscopy

The sample was placed on the stage of an Olympus confocal microscope and excited with 514.5 nm radiation from Coherent model Innova 300 argon ion laser. Scattered light was dispersed and recorded by means of a Dilor XY multichannel Raman spectrometer equipment with a liquid nitrogen-cooled charge-coupled detector. The spectral resolution was 3 $cm^{-1}$. The laser output power at the source was 100–150 mW. The wavenumber range of detection/analysis was from about 200 to 1700 $cm^{-1}$ with 180 s collection time and three accumulations on each sub-region.

## 3. Results and discussion

When viewed under the microscope, each object appeared to have differently coloured regions. The predominant colours on the red shards were black, red and uncoloured; on the gray shards, black and uncoloured and on the teapot, red and uncoloured. This is normally an indication of the composite nature of clay products. A range of spectra were collected from different spots on each sample. The regions with similar colours (e.g. black) were still not homogeneous and did not give the same spectra nor compositions at all times. The spectra as described below were characterized mainly by the presence of quartz, aluminosilicates and pigments [14,15].

### 3.1. São João shipwreck sample

#### 3.1.1. Large red shard

The red and black particles on the large red shard (no. 1) showed the presence of Raman bands at 226, 292, 407, 461, 603, 677, 737, 785, 967, 1021, 1058, 1124, 1163, 1325 and around 1600 $cm^{-1}$ (Fig. 2a–d). The bands at 226(m), 292(s), 407(m)

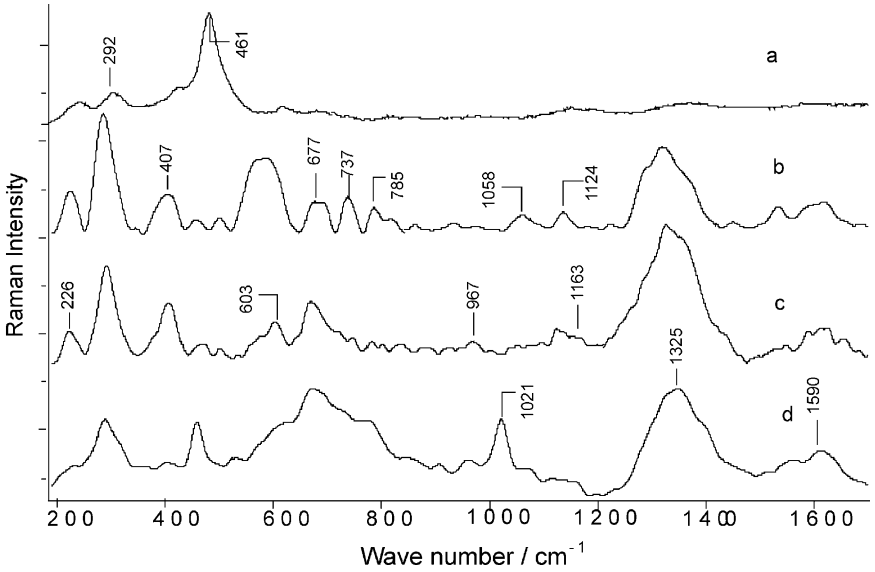


Fig. 2. Representative Raman spectra obtained on large red shard (sample no. 1). Typical components which could be identified were: a—hematite and quartz; b—hematite, kaolin, amorphous aluminosilicates and carbon; c—hematite, anhydrite, quartz and amorphous aluminosilicates and carbon; and d—anhydrite, amorphous aluminosilicates and carbon.

and 603(w) $cm^{-1}$, match closely those of red iron oxide ($\alpha$-$Fe_2O_3$) [12,15,16]. These hematite characteristic bands were previously assigned to $A_{1g}$ (226 $cm^{-1}$), $E_g$ (292 $cm^{-1}$) and $E_g$ (407 and 603 $cm^{-1}$) [16]. Also identified were kaolin bands due to Al–O symmetric stretching at 677 $cm^{-1}$ [14,17], O–H bending vibration at 737 and 785 $cm^{-1}$ and the Al–OH band at around 1124 $cm^{-1}$ [17]. The broad bands in the range 1325–1600 $cm^{-1}$ closely resembled those of amorphous carbon [15,18]. These bands are assigned to the $sp^3$ and $sp^2$ bands of the hybridized carbon, respectively, the so-called D and G bands [19–22]. A ratio of these bands indicates the graphitic content of the amorphous carbon. From the relative intensities of these bands in Fig. 2, it is clear that there is a significantly higher amount of D carbon in the large red shard. This means the amorphous carbon in the sample has a low graphitic content. The uncoloured areas gave high fluorescence background. The 677 $cm^{-1}$ band was very broad and it appeared to comprise the Al–O–Si stretching band (characteristic of kaolins) which normally occurs around 658 $cm^{-1}$ [15]. It is well known that some kaolin clay minerals, particularly kaolinite, show refractory characteristics [12]. Therefore, the detection of its structural O–H bending modes even after firing of the clay product shows that it was not completely decomposed. The appearance of a band resembling that of mullite (967 $cm^{-1}$, Fig. 1c) might mean that the firing occurred above 1200 °C. However, this band shows too low an intensity to be assigned with certainty. The assignment of this band could also be $\nu_1(A_g)$ mode of phosphate ion [3,23,24]. When this band appears together with

the amorphous carbon bands, it suggests that animal bones were used as part of the raw material. On calcinations, bone collagen forms carbon but the inorganic matrix forms phosphate ions with characteristic Raman bands in the region ~965 $cm^{-1}$ [3,23]. This further implies that bone charcoal was used in the kiln as colourant. The sample also shows the strong presence of crystalline quartz characterized by the strong band at 461 $cm^{-1}$. The band at 1058 $cm^{-1}$ could be due to the $\nu_1(A_{1g})$ mode of the carbonate ion [3,24] (Fig. 1a). The band at 1021 $cm^{-1}$ is characteristic of $\nu_1(A_g)$ mode of the anhydrite ($CaSO_4$) [3,25]. The above assignments were confirmed by comparison of the observed spectra with reference data available for hematite, kaolin minerals and amorphous carbon [1,13–15, 16–18,26–29]. The identification of components in this shard is thus certain, except for mullite and the phosphate ion.

### 3.2. São João Baptista shipwreck samples

Two red shards (round, no. 2 and long, no. 3) and two gray shards (large, no. 4 and small, no. 5) from this wreck were investigated.

#### 3.2.1. Round red clay shard

The results obtained for the black and red grains on the round shard showed features of hematite, kaolin, quartz, anhydrite ($CaSO_4$) and amorphous carbon (Fig. 3a–d) as assigned in Table 2. Generally, the spectra of the round red shard shows equal intensity bands at 1351 and 1596 $cm^{-1}$. This is an indication of a more or less equal amount of the $sp^3$ and $sp^2$ (amorphous and graphitic carbon characteristic, respectively) band characteristic in the amorphous carbon. This sample might contain mullite even though the associated band (954 $cm^{-1}$) shows a very low intensity and overlaps the broad bands which are typical of amorphous aluminosilicates. The other possible assignment for this band is phosphate ions [3,23].

#### 3.2.2. Long red clay shard

The Raman spectra of the long clay shard (Fig. 4) also contained features of hematite, quartz, kaolin and amorphous carbon (Table 2). From Fig. 4, it is difficult to ascertain the true characteristics of the amorphous carbon, because some areas show low graphitic carbon (Fig. 4c) and others high graphitic carbon (Fig. 4a, b). Furthermore, the presence of mullite is again uncertain because of the low intensity of the band ascribed to it (958 $cm^{-1}$). The appearance of the 958 $cm^{-1}$ band could also be due to phosphate ion which is closely linked to the amorphous carbon [3,23].

The Raman results showed similar composition for the two red shards (Figs. 3 and 4). The slight differences appeared to be brought about by the presence of additional bands at 1023 $cm^{-1}$. The broadening of 676 $cm^{-1}$ band in Fig. 4 suggests that the crystalline kaolin is distorted to some extent. This band, at 676 $cm^{-1}$, together with the one at 1159 $cm^{-1}$, is rather broad which suggests the presence of amorphous aluminosilicates common in the fired clay products [12]. The band at 1023 $cm^{-1}$ is narrower and high in intensity suggesting the presence of a highly crystalline substance. This feature together with the medium intensity band around

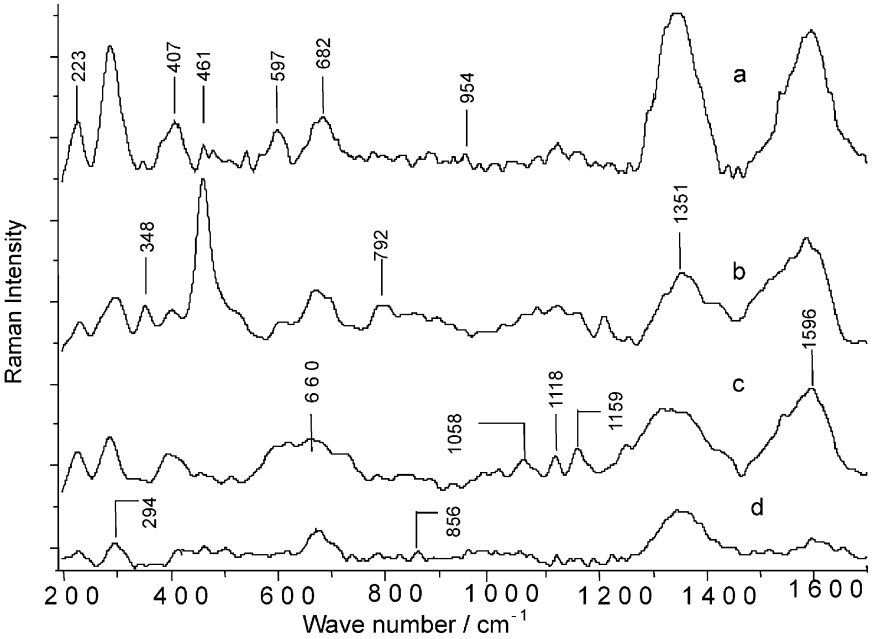


Fig. 3. Representative Raman spectra obtained from the round red shard (sample no. 2). Typical components which could be identified were: a—hematite, kaolin, quartz and amorphous carbon; b—hematite, kaolin, quartz and amorphous carbon; c—hematite, kaolin, amorphous carbon and aluminosilicates; and d—hematite, amorphous carbon and aluminosilicates.

1160 $cm^{-1}$ is characteristic of the anhydrite ($CaSO_4$) [17,25]. The two red shards from the São João Baptista shipwreck show the presence of similar components. Although it is known that kaolin transforms into mullite at higher firing temperature (>1200 °C) [9], the feature around 960 $cm^{-1}$ on these Raman spectra could not be assigned with certainty to mullite because of its weak intensity and the band broadening due to amorphous aluminosilicates. The band at 960 $cm^{-1}$ could also be due to the phosphate ions resulting from the calcinations of animal bones.

### 3.2.3. *Large gray clay shard*

The Raman spectra of the black coloured grains observed on the large gray shard (Fig. 5) showed features of quartz (461 $cm^{-1}$) [12,17], kaolin (679, 1117 $cm^{-1}$) [14], amorphous aluminosilicate (502, ~960 $cm^{-1}$) [10,12,18] and amorphous carbon (1367, 1598 $cm^{-1}$) [15,17,18]. No red regions were observed here under the microscope. The presence of an aluminosilicate glassy phase was manifested by the appearance of broad Raman bands (Fig. 5a–c). In Fig. 5a, the relatively higher amount of G band (1598 $cm^{-1}$) points to the presence of graphitic carbon. The appearance of the band around 965 $cm^{-1}$ suggested the presence of mullite, and this could mean that kaolin was used as part of the raw materials and that the firing temperature exceeded 1200 °C [7]. Alternatively, the 965 $cm^{-1}$ band could be

Table 2
The Raman band assignments of phases in ancient Chinese clay artifacts. The following frequencies ($cm^{-1}$) are a summary of spectra obtained for all different grains/areas on a particular sample

| Large red ($cm^{-1}$) | Round red ($cm^{-1}$) | Long red ($cm^{-1}$) | Clay pot ($cm^{-1}$) | Small gray ($cm^{-1}$) | Large gray ($cm^{-1}$) | Phase | Assignments | References |
|---|---|---|---|---|---|---|---|---|
| 226m | 223m | 227w | 225s | | | H | Fe–O ($A_{1g}$) | [2,11,15,17] |
| | | | | | 268w,b | $CO_3^{2-}$ | C–O | [24,29] |
| 292s | 294s | 295s | 292m | | | H | Fe–O ($E_g$) | [2,11,15,17] |
| | 348w | | 349w | 334w | 335w,b | Q | Si–O | [12] |
| 407m | 407m,b | 407m | 407w | | | H | Fe–O–Fe ($E_g$) | [2,11,15,17] |
| | | | | 417m | | G | $\nu_2(A_g)$ S–O | [24] |
| 461ss | 461ss | 459ss | | 463ss | 461ss | Q | Si–O–Si | [4, 11, 13] |
| | | | | 492w,b | 502b | Al–Si | Si–O ($Q^2 = SiO_2$) | [12,28] |
| | | | | | 571 | | | |
| 603m | 597m,b | 609w | 606w | | | H | Fe–O ($E_g$) | [2,11,15,17] |
| | | | | 621m,b | | Al–Si | Si–O ($Q^2 = SiO_2$) | [12,28] |
| 677m | 682m,b | 676s,b | 676s | 667m | 679s,b | K | Si–O–Al | [11,14,20] |
| 737m | | | | | 743b | K | O–H | [14] |
| 785w | 792w,b | 784m,b | 800s,b | | 772w | K | O–H | [14] |
| | | 822m,b | 823s,b | | | Al–Si | Si–O ($Q^2 = SiO_2$) | [12,28] |
| | | | | | 878w,b | Al–Si | Si–O ($Q^2 = SiO_2$) | [12,28] |
| 967vw | 954vw | 958vw | | 952vw | 965m,b | $M/PO_4^{3-}$ | Si–O/$\nu_1(A_g)$ P–O | [7,10,18,24] |
| | | | | 1007ss | | G | $\nu_1(A_g)$ S–O | [3,25] |
| 1021m | | 1023s | | | 1013b | A | $\nu_1(A_g)$ S–O | [20] |
| 1058m | 1058m | | | | 1076b | $CO_3^{2-}$ | $\nu_1(A_{1g})$ C–O | [3,24] |
| 1124m | 1118m | 1128m,b | | 1121s | 1117w | K | Si–O | [14] |
| 1163w | 1159m | 1159s,b | | 1169s | 1174vw | A and K | S–O and Si–O ($Q^1 = SiO_3$) | [14,26] |
| 1325b | 1351b | 1356b | 1353b | 1358b | 1367b | C | C | [15,18,19] |
| 1590b | 1596b | 1585b | 1589b | 1596b | 1598b | C | C | [15,18,26] |

H, hematite; Q, quartz; K, kaolin; Al–Si, amorphous aluminosilicates; M, mullite; A, anhydrite ($CaSO_4$); G, gypsum; C, amorphous carbon; and $Q^1$ and $Q^2$, $SiO_3$ and $SiO_2$ silica tetrahedral unit with one and two bridging oxygens, respectively.
ss, very strong; s, strong; m, medium; w, weak; and b, broad.

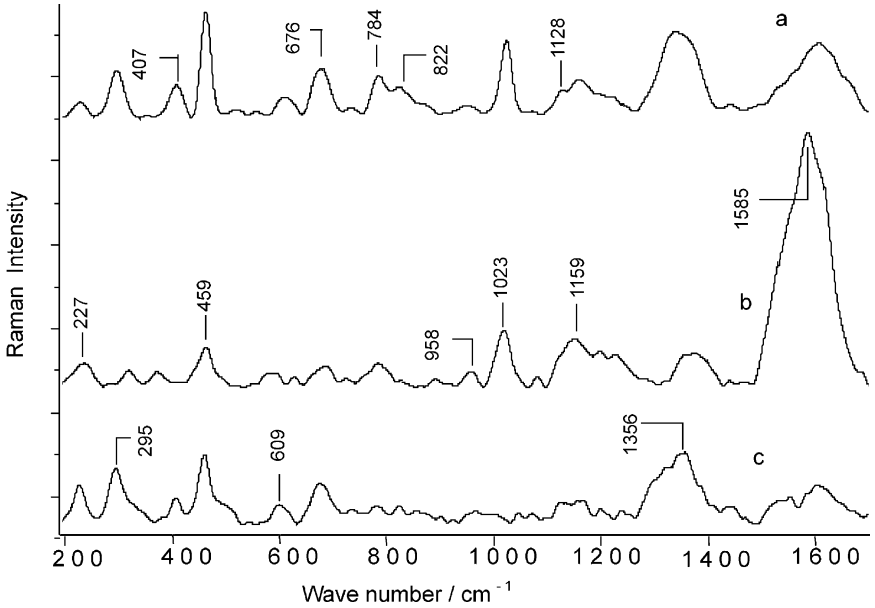


Fig. 4. Representative Raman spectra obtained on long red shard (sample no. 3). Typical components which could be identified were: a—hematite, quartz, kaolin, and amorphous carbon and aluminosilicates; b—kaolin, quartz, mullite, anhydrite, amorphous aluminosilicates and carbon; and c—hematite, quartz and amorphous carbon.

due to the phosphate ions that resulted from the calcinations of carbon source (possibly animal bones). Fig. 5a further shows a band around 1013 $cm^{-1}$ (even though slightly lower) which is closest to the $\nu_1(A_g)$ mode in anhydrite ($CaSO_4$) [3,24]. The assignment of the band at 1076 $cm^{-1}$ is uncertain. The authors suggest this band to be due to the $\nu_1(A_{1g})$ carbonate mode particularly when it is accompanied by the band at 268 $cm^{-1}$ [3,23,29]. The band at 571 $cm^{-1}$ could not be assigned.

### 3.2.4. *Small gray clay shard*

The Raman spectrum obtained from some black grains of the small clay shard (Fig. 6b) is dominated by broad features throughout the frequency range of analysis (200–1700 $cm^{-1}$). This suggested the presence of amorphous rather than crystalline aluminosilicates. However, the bands appearing above the broad features around 1120 $cm^{-1}$ suggested that kaolin clay mineral was used as part of the raw materials [14]. The analysis of other black grains (Fig. 6a, b) confirms the presence of kaolin, indicated by bands at 667 and 1121 $cm^{-1}$ [10: p. 129]. The intense and narrow band around 463 $cm^{-1}$ (Fig. 6c) indicated the presence of crystalline quartz ($\alpha$-$SiO_2$) [12]. No red grains were observed. The characteristic bands of amorphous carbon (1358, 1596 $cm^{-1}$) were also evident (Fig. 6a–c). In Fig. 6, the relatively higher amount of G band (1598 $cm^{-1}$) points to the presence of a significant amount of graphitic car-

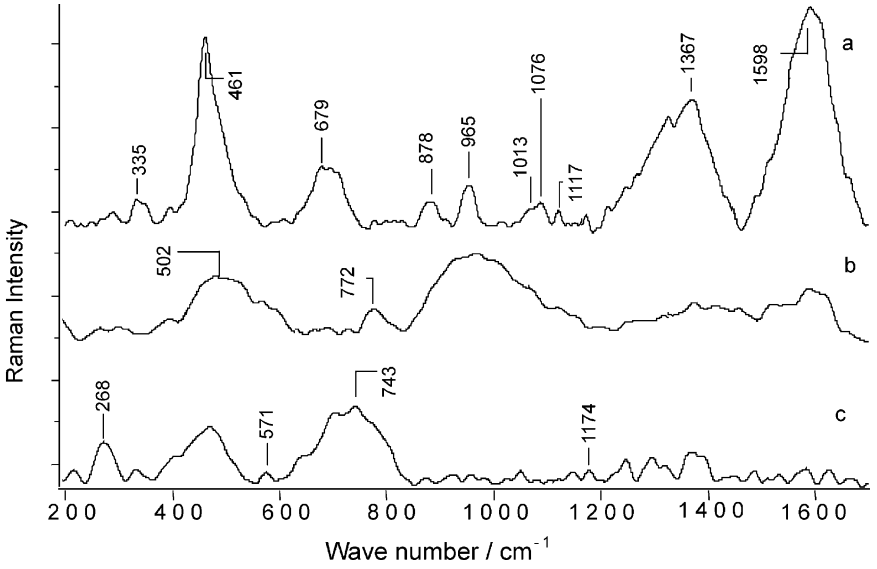


Fig. 5. Representative Raman spectra obtained on large gray shard (sample no. 4). Typical components which could be identified were: a—quartz, kaolin, mullite, anhydrite and amorphous carbon; b—amorphous aluminosilicates and kaolin; and c—kaolin and amorphous aluminosilicates.

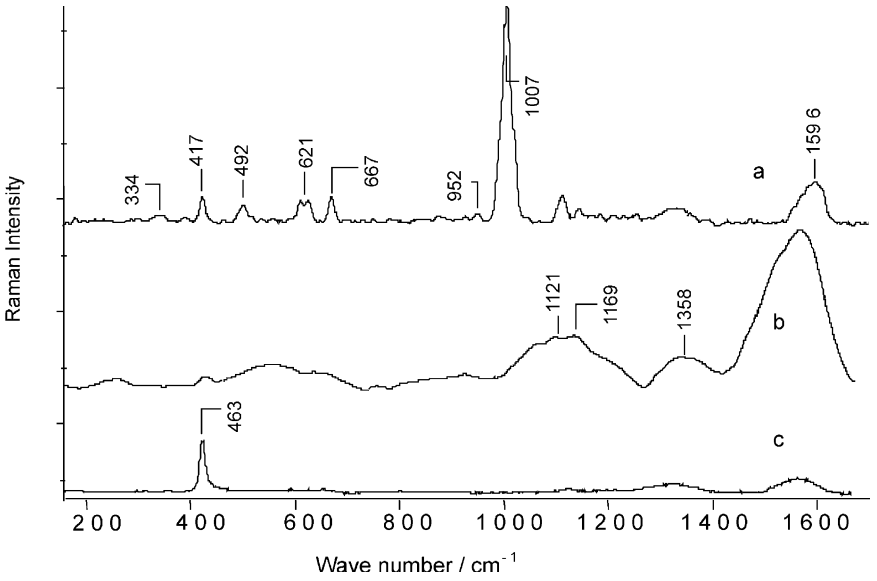


Fig. 6. Representative Raman spectra obtained on small gray shard (sample no. 5). Typical components which could be identified were: a—quartz, kaolin, mullite, anhydrite and amorphous carbon and aluminosilicates; b—kaolin, amorphous aluminosilicates and carbon; and c—quartz and amorphous carbon.

bon. The weak band appearing at 952 $cm^{-1}$ (Fig. 6a) could be due to mullite or phosphate ions, but as a result of the weak intensity and broadening this assignment is uncertain. The most intense and narrow band appears at 1007 $cm^{-1}$ in Fig. 6a. The bands in this region have previously been associated with the presence of $\nu_1(A_g)$ modes in gypsum ($CaSO_4 \cdot 2H_2O$) [3,25]. This assignment is further confirmed by the presence of $\nu_2(A_g)$ for gypsum at 417 $cm^{-1}$ [24]. The Raman spectra of the uncoloured areas resulted in a high fluorescence background.

The Raman spectra of the above two gray clay shards showed no features of red iron oxides. The spectral features pointed to similar components for the two samples.

### 3.3. *Red clay pot of Chinese origin*

The object contained only red grains and uncoloured areas when viewed under the microscope. The spectra of the red grains showed features of hematite, kaolin, amorphous aluminosilicates and carbon (Fig. 7 and Table 1). The broadening of the bands appear to be due to the presence of amorphous aluminosilicate. The unusually lower intensity and broadening in the region of quartz could either be due to its low content or to its absence in free and crystalline form. The analysis on clear areas of the clay pot resulted in high fluorescence background.

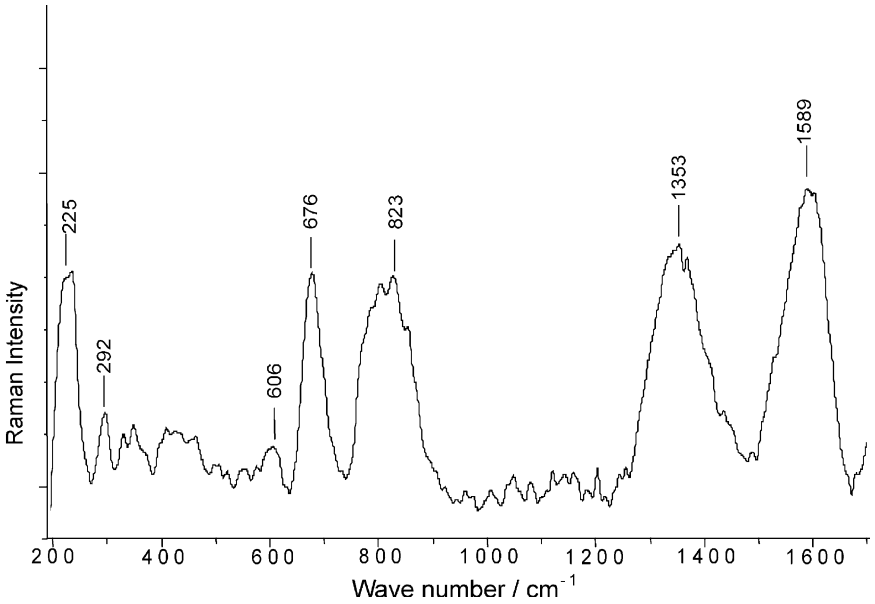


Fig. 7. Representative Raman spectrum obtained on the red clay pot (sample no. 6). Typical components identified were hematite, quartz, kaolin, amorphous aluminosilicates and carbon.

## 4. Conclusion

The three red clay shards (Fig. 1, sample nos. 1–3) have similar compositions characterized by the presence of kaolin, quartz, hematite, amorphous aluminosilicates and carbon. The spectrum from the red clay teapot (Fig. 1, sample no. 6) showed the presence of kaolin, hematite, amorphous aluminosilicates and carbon. The differences in the spectral features (including the absence of quartz bands in the clay teapot spectrum) of red clay shards and clay teapot are confirmed by the different visual appearances of the two sets of samples. The clay teapot appears to be more homogeneous than the red shards. The colouring materials (pigments) used on the red shards and clay teapot were hematite (red) and amorphous carbon (black). The gray clay shards (Fig. 1, sample nos. 4 and 5) showed the presence of kaolin, quartz, amorphous aluminosilicates and carbon. The colouring material or pigment detected on the gray shards was amorphous carbon with strong graphitic characteristics. The lack of iron oxides in the gray artifacts set them apart from the red artifacts.

There could be few reasons for the appearance of amorphous carbon in the finished (fired) clay products. Since clay artifacts are formed at higher temperatures, far above which carbon is likely to occur, the observed carbon could be originating from the firing (under reducing atmosphere) of some organic substance in the starting mixture or from colouring materials that could have been applied after the firing process [15]. It could also be that the raw material contained some carbon source (e.g. animal bones) which on firing in air resulted in amorphous carbon and phosphate ions. However, it is difficult to tell which method was used by simply looking at the samples.

All samples showed, in addition, the features resembling those of mullite, phosphates and carbonate ions, however, their presence could not be ascertained conclusively from the Raman spectroscopic results. The study has proven that differentiation (by Raman spectroscopy) between the present clay artifacts is based mainly on the colouring materials used. It follows that Raman spectroscopy can be used non-destructively to successfully identify crystalline and non-crystalline phases (including colouring materials) constituting the clay artifacts. In the present case, the only applicable technique was Raman spectroscopy because of its availability and non-destructive nature, as the samples used in this study were museum artifacts and could not be subjected to destructive techniques.

## Acknowledgements

The financial support by the National Research Foundation in Pretoria and the University of Pretoria is gratefully acknowledged. The authors thank the J A van Tilburg museum curator Dr Valerie Esterhuizen for the supply of samples and historical information.

## References

[1] R.J.H. Clark, M.L. Curri, J. Mol. Struct. 440 (1998) 105.
[2] C.S. Nurlbut Jr., C. Klein, Manual of Mineralogy, 19th ed., John Wiley & Sons Inc, New York, 1971.
[3] H.G.M. Edwards, E.M. Newton, J. Russ, J. Mol. Struct. 550–551 (2000) 245.
[4] L. Burgio, R.J.H. Clark, Spectrochim. Acta 57A (2001) 149.
[5] S.P. Best, R. Withnall, Endeavour 16 (1992) 66.
[6] M.J. Wilson, Clay Mineralogy: Spectroscopic and Chemical Determinative Methods, Chapman & Hall, London, 1994.
[7] N. Palmgren, W. Steger, N. Sundius, Sung Sherds, Almovist & Wilksell, Stockholm, 1963, pp. 380.
[8] P. Colomban, J. Mater. Sci. 24 (1989) 3011.
[9] N. Palmgren, W. Steger, N. Sundius, Sung Sherds, Almovist & Wilksell, Stockholm, 1963.
[10] P. Valfre, Yixing Teapots for Europe, Exotic line, Janvier 2000, (China).
[11] P. Colomban, G. Sagon, X. Faurel, J. Raman Spectrosc. 32 (2001) 351.
[12] D. Bikiaris, S. Daniila, S. Sotiropoulou, O. Katsimbiri, E. Poulidou, A.P. Moutsatsou, Y. Chryssoulakis, Spectrochim. Acta Part A 56 (1999) 3.
[13] N.Q. Liem, G. Sagon, V.X. Quang, H. Van Tan, P. Colomban, J. Raman Spectrosc. 31 (2000) 933.
[14] P. Colomban, F. Treppoz, J. Raman Spectrosc. 32 (2001) 93.
[15] J. Zuo, C. Xu, C. Wang, Z. Yushi, J. Raman Spectrosc. 30 (1999) 1053.
[16] L.A. De Faria, S.V. Silva, M.T. De Oliviera, J. Raman Spectrochim. 28 (1997) 873.
[17] R.L. Frost, P.M. Fredericks, J.R. Bartlett, Spectrochim. Acta 49A (5–6) (1993) 667.
[18] I.M. Bell, R.J.H. Clark, P.J. Gibbs, Spectrochim. Acta 53A (1997) 2159.
[19] M. Tabbal, T. Christidis, S. Isber, M.A. El Khakani, P. Mérel, M. Chaker, Thin Solid Films 453–454 (2004) 234.
[20] J.C. Orlianges, C. Champeaux, A. Catherinot, Th. Merle, B. Angleraud, Thin Solid Films 453–454 (2004) 285.
[21] K. Lee, H. Sugimura, Y. Inoue, O. Takai, Diamond Relat. Mater. 13 (3) (2004) 507.
[22] R.N. Tarrant, D.R. McKenzie, M.M.M. Bilek, Diamond Relat. Mater., in press.
[23] I.A. Degen, G.A. Newman, Spectrochim. Acta Part A 49 (5–6) (1993) 859.
[24] V.C. Farmer, Infrared spectroscopy, in: H. van Olphen, J.J. Fripiat (Eds.), Data Handbook for Clay Materials and Other Non-metallic Minerals, Pergamon, Oxford, 1979.
[25] C.H. Chio, S.K. Sharma, D.W. Muenow, Am. Miner. 89 (2004) 390.
[26] R.J.H. Clark, Chem. Soc. Rev. 24 (1995) 187.
[27] V.C. Farmer, The Infrared Spectra of Minerals, Mineralogical Society, London, 1975.
[28] E.C. Ziemath, M.A. Aegeter, J. Mater. Res. 9 (1994) 216.
[29] R. Burch, C. Passingham, G.M. Warnes, D.J. Rawlence, Spectrochim. Acta 46A (1990) 243.